GPS Solutions (2021) 25:131
https://doi.org/10.1007/s10291-021-01168-1

ORIGINAL ARTICLE

Initial Assessment of the BDS-3 PPP-B2b RTS compared with the CNES RTS

Jun Tao[1] · Jingnan Liu[2,3] · Zhigang Hu[2,3] · Qile Zhao[2,3] · Guo Chen[2] · Boxiao Ju[2]

Received: 8 January 2021 / Accepted: 20 July 2021 / Published online: 29 July 2021

Abstract

In 2020, the BeiDou navigation satellite system (BDS) initiated a real-time service (RTS) for precise point positioning (PPP) using the B2b signal for users in China and its surrounding areas. A decimeter-level accuracy is expected to be achieved using a single receiver. In this study, the PPP-B2b service is experimentally analyzed based on 7 days of corrections and compared with the RTS provided by the Centre National d'Etudes Spatiales (CNES). The availability and completeness of these two RTS products are first evaluated based on the quality of the observation-specific bias (OSB), the satellite orbit and clock offset products. The signal-in-space ranging error (SISRE) is also calculated and evaluated. PPP-B2b can provide stable service in Asia and has better availability and completeness for BDS-3 than does CNES, though the opposite is true for GPS. The analysis reveals a nonnegligible constant satellite-specific bias in the PPP-B2b clock offset for GPS and a smaller bias for BDS-3; this bias is absent in the CNES products. The SISREs of the PPP-B2b products are affected by this bias, but the SISRE STD is comparable to that of the CNES products. Positioning experiments are carried out for the PPP-B2b and CNES products using six stations evenly distributed across China. The kinematic PPP results of BDS-3-only positioning, achieving accuracy at the centimeter level using PPP-B2b, are in good agreement with the GPS-only results using CNES. The abnormal average convergence time exceeding 60 min for GPS confirms that the satellite-specific bias in the PPP-B2b clock offset degrades the pseudorange accuracy, which should be improved in the near future.

Introduction

The construction of the third generation of the BeiDou navigation satellite system (BDS-3) was initialized in 2009 with the aim to improve the performance further and expand the functions of BDS-2. After the verification of five experimental satellites with new payloads, newly designed signals and new techniques (Yang et al. 2018), the first two medium earth orbit (MEO) satellites for BDS-3 were successfully launched at the end of November 2017. At the end of December 2018, BDS-3 provided global positioning, navigation and timing (PNT) services with 18 MEO satellites and 1 geostationary orbit (GEO) satellite in orbit (CSNO 2018). On July 31, 2020, the full BDS-3 constellation was completed, including 3 GEO, 3 inclined geosynchronous orbit (IGSO) and 24 MEO satellites, providing global users with positioning, timing and velocity accuracies of 10 m, 20 ns and 0.2 m/s, respectively (CSNO 2019a).

In terms of signal frequency, BDS-2 satellites transmit legacy B1I (1561.098 MHz) and B3I (1268.520 MHz) signals, while BDS-3 satellites add three new public signals: B1C (1575.42 MHz), B2a (1176.4 MHz) and B2b (1207.14 MHz) (CSNO 2017a, 2017b, 2020a). The pseudorange quality of these new signals is significantly improved compared to that of the signals transmitted by the BDS-2 satellites. Moreover, unlike BDS-2 there is no satellite-induced code bias in BDS-3, which is more conducive for wide-lane ambiguity resolution (Zhang et al. 2017; Xie et al. 2017; Yang et al. 2018; He et al. 2020). Furthermore, each BDS-3 satellite uses a passive hydrogen maser (PHM) as a frequency standard for navigation signals, thereby exhibiting higher stability and higher prediction accuracy for the

✉ Zhigang Hu
zhigang.hu@whu.edu.cn

Jingnan Liu
jnliu@whu.edu.cn

[1] School of Geodesy and Geomatics, Wuhan University, No. 129 Luoyu Road, Wuhan 430079, China

[2] GNSS Research Center, Wuhan University, No. 129 Luoyu Road, Wuhan 430079, China

[3] Collaborative Innovation Center of Geospatial Technology, Wuhan University, No. 129 Luoyu Road, Wuhan 430079, China

onboard atomic clocks than BDS-2 (Wu et al. 2018; Xie et al. 2017; Lv et al. 2018). In addition, pairing an inter-satellite link (ISL) terminal with a BDS-3 satellite creates a 'bridge' for communication and measurements between satellites, which improves the orbit-only signal-in-space ranging error (SISRE) by approximately 37–76% for different satellites compared with ground-tracking orbit determination (Yang et al. 2017). Consequently, centimeter-level and decimetre-level accuracies can be achieved using ISL data for orbit determination on MEO and IGSO satellites, respectively (Tang et al. 2018; Xie et al. 2020). BDS-3 can further achieve more stable autonomous navigation performance (Guo et al. 2020) by introducing ISL measurements into the BDS-3 ground operation control (Liu et al. 2019), which significantly improves the SISREs for broadcast ephemerides compared with BDS-2 (Zhang et al. 2019; Lv et al. 2020; Shi et al. 2020; Yang et al. 2020).

For many years, precise point positioning (PPP) technology has been limited to the post-processing mode due to the large delay in the availability of precise satellite orbit and clock products. To meet the needs of real-time positioning, real-time service (RTS) for PPP was announced by the International GNSS Service (IGS) in 2013 based on the multi-GNSS experiment (MGEX) (Montenbruck et al. 2017). Users can retrieve real-time state-space representation (SSR) corrections for different products, such as precise orbit, clock and code biases encoded in the Radio Technical Commission for Maritime Services (RTCM) protocol via BNC software or RTKLIB. Such products are currently provided by several analysis centers, such as Deutsches GeoForschungsZentrum (GFZ), the Center for Orbit Determination in Europe (CODE), the Centre National d'Etudes Spatiales (CNES) and Wuhan University (WHU). An early evaluation confirmed that RTS should provide data at high-rate update intervals (5 or 10 s) and that obsolete data should be excluded at the client (Hadas and Bosy 2015). Kazmierski et al. (2018) further assessed the availability and quality of CNES RTS products and verified that the proper weighting of observations considering the qualities of real-time orbit and clock products in stochastic models improves the positioning performance. Furthermore, the evolution of the CNES RTS was evaluated over the 3-year period between 2017 and 2020, and the availability of GPS, GLONASS, Galileo and MEO satellites for BDS real-time corrections exceeded 95% in 2019 (Kazmierski et al. 2020). Wang et al. (2019) investigated the BDS-2-only real-time precise point positioning (RTPPP) performance by using the CNES RTS. They achieved centimeter-lever and decimeter-level static and kinematic mode accuracies, respectively, using ten MGEX stations. With the incorporation of BDS-3 satellites, better PPP solutions can be achieved than with BDS-2 satellites alone (Zhang et al. 2020; Shi et al. 2020; Pan et al. 2020), but the performance is still worse than with the inclusion of only GPS satellites, probably due to the worse quality of the correction products (Pan et al. 2020).

To meet the demands of RTPPP, BDS-3 also provides a RTPPP service on the B2b signal utilizing a regional network of tens of stations. Three BDS-3 GEO satellites are used to broadcast the same corrections for visible regional satellites in Asia, with intervals of 6 s for clock offset products and 48 s for orbit products (CSNO 2020b). Similar systems include the High-Accuracy Services (HAS) provided by Galileo and Centimeter-Level Augmentation Service (CLAS) provided by Japan's Quasi-Zenith Satellite System (QZSS). The binary format for PPP-B2b corrections is defined in the interface control document (ICD), making it possible to achieve the decimeter-level positioning accuracy of a single receiver (CSNO 2019b). Early results show that PPP-B2b can stably provide PPP services for satellites in the Asia–Pacific region (Lu et al. 2020). However, the PPP-B2b service performance remains unknown since the receiver manufacturer does not fully support the format. Hence, in this study, we collect corrections received from B2b signals and analyze the products in comparison with CNES products.

First, we briefly describe the message type and the ephemeris matching strategy provided in the PPP B2b signal. We present the dataset used herein and its visibility, availability and completeness during the analysis period. Then, the product is assessed with the PPP validation strategy. Next, we evaluate the observation-specific bias (OSB), orbit and clock offset products provided by the PPP-B2b service and compare them with those offered by the CNES service. Positioning experiments are further carried out for validation. Finally, our conclusions and findings are summarized.

Data collection

The PPP-B2b signal format is now available online (http://www.beidou.gov.cn/xt/gfxz/202008/P020200803362062482940.pdf), and the service is free to users. We employ a single receiver that we deployed in Wuhan to receive the SSR corrections to assess the performance of the PPP-B2b service. The binary data are decoded, and the precise products are restored according to the PPP-B2b signal ICD. In this section, the visibility, availability and completeness of the corrections are evaluated in comparison with CNES products.

Matching strategy

The PPP-B2b signal broadcasts both the I-component and the Q-component, whereas the first three BDS-3 GEO satellites broadcast only the I-component (CSNO 2020b).

Hence, the PPP-B2b corrections are modulated and broadcast through these three GEO satellites. Table 1 lists several message types defined in the PPP-B2b signal ICD. The clock corrections are broadcast every 6 s, while the other messages are updated every 48 s. The orbit and clock corrections refer to the CNAV1 navigation messages of the BDS-3 B1C signal and the legacy navigation (LNAV) messages of GPS.

To ensure that the information contents of different message types are inter-related, four issue of data parameters (IODPs) are defined: IOD SSR, IODP, IODN and IOD Corr. IOD SSR indicates the issue number in the SSR data, and corrections with a different IOD SSR should not be used together. IODP indicates the issue number of the type 1 satellite mask, which is used to match message types 4, 5 and 6. IODN indicates the issue number of corrections and broadcast ephemeris; this parameter is included in message type 2, and users can use IODN to match clock and orbit corrections with ephemeris to recover precise products. IOD Corr indicates the issue number of orbit and clock corrections; this parameter is included in message types 2, 4, 6 and 7. Users should first match the clock corrections with the orbit using IOD Corr and then obtain the corresponding IODN value to recover precise satellite clock offsets.

Table 1 Nominal validity of different message types broadcast in the PPP-B2b signal

Information content	Message type	Update interval (s)	Nominal validity
Satellite mask	1	48	–
Orbit correction	2,6,7	48	96
Differential code bias	3	48	86,400
Clock correction	4,6,7	6	12
User range accuracy index	2,5,6,7	48	96

Dataset

PPP-B2b corrections were collected for a time span of one week from day of year (DOY) 238 to DOY 244 in 2020, a month after the BDS-3 PPP-B2b service announcement. Figure 1 illustrates the workflow of the PPP-B2b correction recovery procedure. The binary data are decoded successfully with homemade software according to the ICD (CSNO 2020b), and together with CNAV1 and LNAV navigation messages, precise orbit and clock products are recovered. Corrections provided by CNES are also received and saved in files during the same period using a BNC client. OSB, precise satellite orbit and satellite clock offset products provided by the PPP-B2b and CNES services are restored and saved in RINEX format. Then, we use these files as inputs in our study.

At present, the PPP-B2b service generally provides products for GPS and BDS-3 satellites (C19–C46), while CNES provides corrections for GPS/GLONASS/GALILEO/BDS satellites (C01–C37). Services are not available for satellites C38–C46, since the tracking stations are not sufficient to determine their orbits at the moment. Therefore, this study investigates and compares only the products for the common GPS and BDS-3 satellites (C19–C37) between PPP-B2b and CNES.

Visibility

To determine the accurate coverage of the PPP-B2b service, we compare the theoretically visible satellites covering all of earth with the satellites provided in the PPP-B2b products. A common area means that the PPP-B2b service has visibility in that area. The only satellites that count are those with both orbit and clock products recovered successfully utilizing PPP-B2b corrections within the nominal validity conditions of $\Delta t_{clk} \leq 12s$, $\Delta t_{orbit} \leq 96s$ recommended by the PPP-B2b signal ICD. The average common satellite numbers over

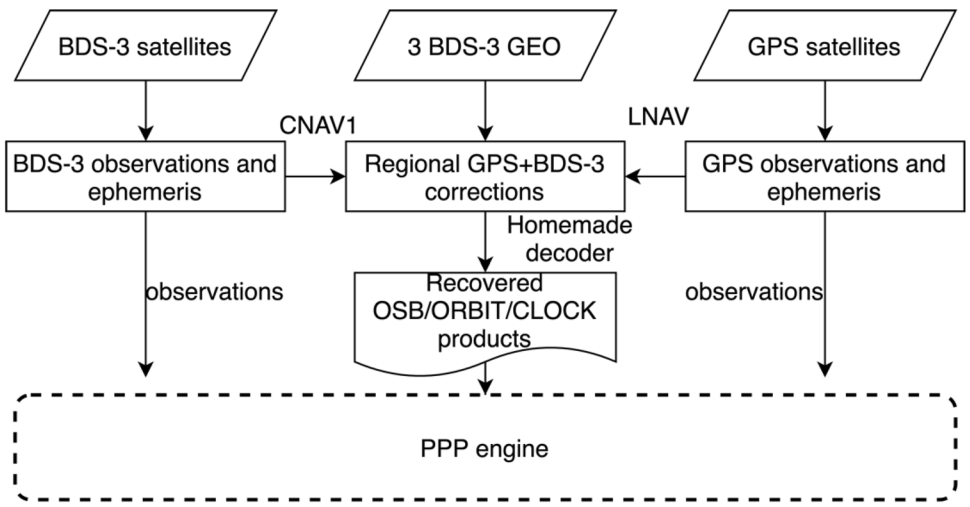

Fig. 1 Flowchart of the PPP-B2b correction recovery procedure on the user side. The binary corrections are decoded using a homemade software, PPP-B2b precise products are recovered then with the help of the CNAV1 and LNAV navigation messages

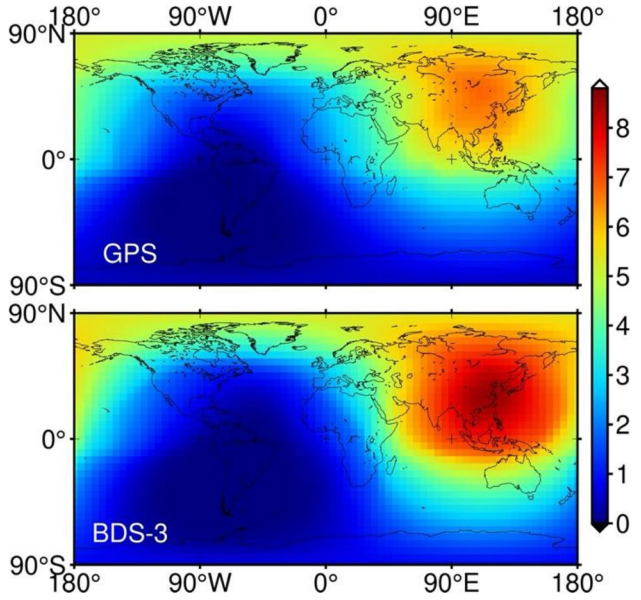

Fig. 2 Average numbers of matched GPS and BDS-3 satellites for PPP-B2b corrections

the grid calculated for GPS and BDS-3 during the analysis period are depicted in Fig. 2. The PPP-B2b service coverage is relatively even across all of Asia, with the best coverage of eastern China, where users can match 8 and 6 satellite corrections for BDS-3 and GPS, respectively. It is worth mentioning that the low number of satellites with average visibility is mainly due to the mismatched clock corrections instead of the orbit corrections. The PPP-B2b service can also be used in some parts of Europe; however, compared to Asia, the satellite elevations and the number of satellites are worse, resulting in an unsatisfactory PPP performance.

Availability and Completeness

For RTPPP, the interruption and incompleteness of SSR corrections seriously impact the positioning accuracy (Hadas and Bosy 2015). Prior to assessing the quality, we first analyze the availability and completeness of the products. The availability can be calculated as $P_{availability} = N_{valid}/N_{all}$, where N_{valid} and N_{all} represent the number of epochs that can match the corresponding orbit and clock corrections within the nominal validity and the number of all epochs, respectively. Likewise, the completeness can be calculated as $P_{completeness} = N_{matched}/N_{theory}$, where $N_{matched}$ and N_{theory} represent the matched number of satellites in corrections and the theoretical number of satellites in the visible region with an elevation cut-off of 10 degrees during the analysis period, respectively. For this assessment, we simulate a receiver in eastern China, where the best enhancement is acquired with the PPP-B2b service, and we analyze its availability and completeness for that week.

As depicted in Fig. 3, the average PPP-B2b availabilities for BDS-3 and GPS are 97.5% and 91.5%, respectively. The reason for the lower GPS availability is that GPS corrections are frequently lost during 22:00–24:00 each day, while BDS-3 corrections are received normally during this period. The average PPP-B2b product completeness for BDS-3 is 92%, while that for GPS is only 72%, which can also be inferred from the average numbers of satellites in Fig. 2. The reason may be the bandwidth limitations of the B2b signal, which requires PPP-B2b to provide BDS-3 corrections with higher priority and cut the GPS signal if the data exceed the capacity. Compared with PPP-B2b, CNES provides a more continuous service for internet users, and the availability and completeness for GPS are 100%, while for BDS-3, the availability and completeness are 94.68% and 92.82%, respectively, due to missing products on days 1, 6 and 7, respectively.

Product assessment

The PPP-B2b and CNES products are assessed by differencing the corrections with the MGEX final products. The global average SISRE can then be computed using orbit and clock errors. Note that the orbit and clock references between the final products and PPP-B2b products are different, and datum discrepancies should be pre-corrected before the evaluation. For the clock comparison, since the PPP-B2b signal broadcasts only regional corrections for GPS and BDS-3, the reference satellite in the double-difference (DD) process will change when that satellite is not visible in the regional GNSS network, leading to a system bias in that satellite's DD series. This datum jump should be corrected first when evaluating the standard deviation (STD) statistic.

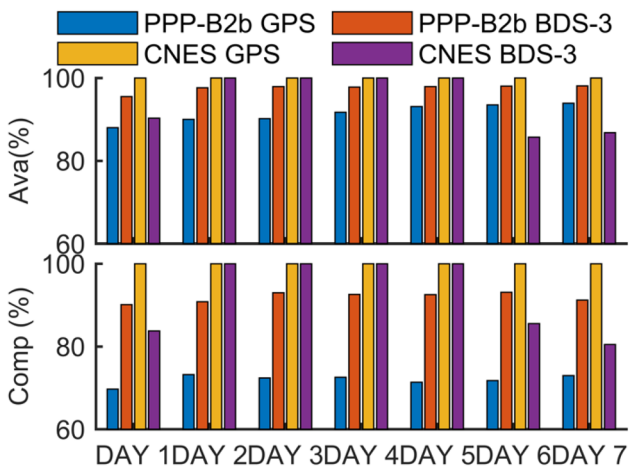

Fig. 3 Availability (top panel) and completeness (bottom panel) of PPP-B2b and CNES products

SISRE computation

The instantaneous SISRE refers to the SISRE in the user's line of sight caused by the satellite orbit error and the satellite clock error, usually related to the user's location on earth. The global average SISRE is computed for a statistical analysis of all the instantaneous SISREs for all of earth and all epochs and is expressed as:

$$\mathrm{SISRE} = \mathrm{rms}\left(\sqrt{\left(a_1 dR - \delta\mathrm{clk}\right)^2 + a_2\left(dA^2 + dC^2\right)}\right) \quad (1)$$

where dR, dA and dC are the orbit errors in the radial, along-track and cross-track (RAC) directions, respectively, and a_1 and a_2 are the SISRE weight coefficients related to the altitude of the satellite within the constellation with values of 0.98 and 1/49 for GPS, respectively, and 0.98 and 1/54 for BDS-3 (Montenbruck et al. 2015). Due to the correlation between the satellite orbit and clock, the SISRE will generally be smaller than the sum of the errors caused by the satellite orbit error and the clock offset (Montenbruck et al. 2015). To determine the contributions of the different components, orbit-only SISREs can also be computed according to:

$$\mathrm{SISRE}_{orbit} = \mathrm{rms}\left(\sqrt{a_1 dR^2 + a_2\left(dA^2 + dC^2\right)}\right) \quad (2)$$

To evaluate the PPP-B2b and CNES RTS products, we adopt multi-GNSS products of WHU (WUM) as a reference. The satellite orbit accuracy is at the centimeter level, and satellite clock offset accuracy is approximately 0.1 ns (Guo et al. 2016). Differential code bias (DCB) products are evaluated by comparing the corrections with the MGEX DCB products generated by the University of the Chinese Academy of Sciences (CAS), and the stability of the DCB products over one month is approximately 0.11 ns for GPS, 0.18 ns for GLONASS, 0.17 ns for BDS and 0.14 ns for Galileo (Wang et al. 2016). The reference points of the precise satellite orbit and clock products are consistent between CNES and WUM but different from PPP-B2b. Therefore, systematic biases should be removed before evaluating the PPP-B2b products.

The Beidou Coordinate System (BDCS) adopted by the BDS is aligned with the latest International Terrestrial Reference Frame (ITRF). In addition, BDS Time (BDT) is used as the time reference for BDS, and thus, an offset of 14 s compared with GPS System Time (GPST) should be corrected during preprocessing (CSNO 2019a). The PPP-B2b signal provides the antenna phase center (APC) satellite position of the B3 signal for BDS-3 and the L1/L2 ionosphere-free (IF) combination APC satellite position for GPS, which is different from the center-of-mass (CoM) satellite position provided by reference WUM products. A correction for the platform center offset (PCO) should be employed in the PPP-B2b products utilizing the PCO information provided in the ICD. The formula can be expressed as:

$$r^{\mathrm{j}}_{\mathrm{APC}} = r^{\mathrm{j}}_{\mathrm{CoM}} + A^{\mathrm{T}} \cdot a^{\mathrm{j}}_{\mathrm{pco}} \quad (3)$$

where r^j_{APC} and r^j_{CoM} represent the satellite APC position and CoM position, respectively, a^j_{pco} represents the PCO correction for satellite j and A represents the satellite attitude matrix (Montenbruck et al. 2015). For clock corrections, both PPP-B2b and WUM GPS satellite clock offsets refer to the L1/L2 IF combination. However, PPP-B2b provides satellite clock products in reference to the B3 signal, which differs from WUM products computed from B1/B3 IF observations. To reach a consistent datum, the DCB should be taken into consideration before an assessment. Similar to time group delays broadcast in navigation messages, PPP-B2b provides OSB products to compensate for the inter-frequency bias for different signals. These OSB products are used to convert the satellite clock offsets to the B1/B3 datum, and the formula can be expressed as:

$$dt^{\mathrm{j}}_{\mathrm{IF_{B1B3}}} = dt^{\mathrm{j}}_{\mathrm{B3}} - \frac{f_1^2}{f_1^2 - f_3^2} \cdot b^{\mathrm{j}}_{\mathrm{B1B3}} \quad (4)$$

where $dt^j_{IF_{B1B3}}$ represents the satellite clock offset for IF_{B1B3} observations for satellite j, f_1 and f_3 represent the B1 and B3 frequencies, respectively, and b^j_{B1B3} represents the DCB between B1 and B3.

Clock evaluation

Precise WUM products are used as the reference for the clock evaluation. By comparing the RTS solutions with the final WUM products, the single-difference (SD) values between the two clock products can be acquired, but a systematic bias that affects all satellites of a constellation, in the same manner, remains in the SD series. It is generally caused by the realization of the GNSS-specific system time scales in different analysis centers (Montenbruck et al. 2015). Typically, the DD method is adopted to reduce this bias by selecting a reference satellite or correcting the difference computed in each epoch from the average SD values of satellites in a constellation (Montenbruck et al. 2015):

$$\nabla\Delta C^s_{a,b} = (C^s_a - C^s_b) - \frac{1}{M}\sum_{i=1}^{M}(C^i_a - C^i_b) \quad (5)$$

where $\nabla\Delta$ is the DD operator, C represents the clock error and $\nabla\Delta C^s_{a,b}$ represents the DD value between the SD values of products a and b for satellite s with respect to the average $\frac{1}{M}\sum_{i=1}^{M}(C^i_a - C^i_b)$, in which M is the number of satellites. The STD and root mean square (RMS) of the DD clock series can

be used to evaluate the accuracy of clock products, where the STD reflects the PPP positioning accuracy after convergence and the RMS generally affects the convergence time of PPP positioning. However, for PPP-B2b products, only regional satellites can be received in each epoch. Hence, the navigation satellites generally ascend or descend relative to the regional GNSS network; the average of SD values also changes, resulting in discontinuous satellite DD series. As a consequence, the STD statistic is severely affected. To properly assess the accuracy of regional clock products, this study applies the following formula to re-edit the DD series:

$$\nabla\Delta C^{s}_{t,(a,b)} = \nabla\Delta C^{s}_{t,(a,b)} - \Delta D_{t,t-1} \tag{6}$$

$$\Delta D_{t,t-1} = \begin{cases} \frac{1}{M}\sum_{i=0}^{M}\Delta\nabla\Delta C^{i}_{t,t-1(\mathrm{a,b})}, & abs\left(\frac{1}{M}\sum_{i=0}^{M}\Delta\nabla\Delta C^{i}_{t,t-1(\mathrm{a,b})}\right) \geq 0.1ns \\ 0 & abs\left(\frac{1}{M}\sum_{i=0}^{M}\Delta\nabla\Delta C^{i}_{t,t-1(\mathrm{a,b})}\right) < 0.1ns \end{cases} \tag{7}$$

where $\Delta\nabla\Delta C^{i}_{t,t-1(\mathrm{a,b})}$ represents the time difference of $\nabla\Delta C^{i}_{t,(a,b)}$ between epochs t and t-1 for satellite i. The DD clock series is re-edited to compensate the systematic error when the average value of the $\Delta\nabla\Delta C^{i}_{t,t-1(\mathrm{a,b})}$ of all satellites is more than $\pm 0.1ns$.

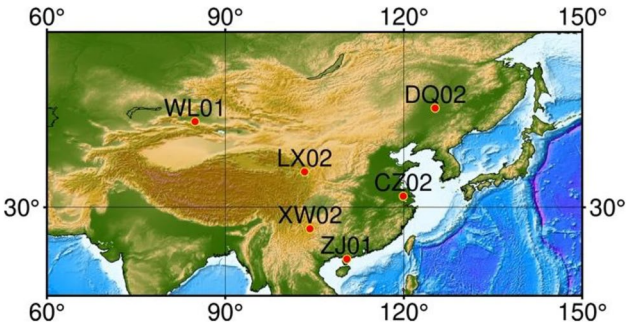

Fig. 4 Distribution of the six stations for PPP experiments

PPP validation

To study the positioning performance of PPP-B2b products, six multi-GNSS tracking stations distributed across China are selected, as depicted in Fig. 4. These stations are equipped with TRIMBLE BD990 and UNICORE ub4b0 receivers, both of which fully support the BDS-3 constellation. The reference coordinates are computed by three days of static PPP with an accuracy reaching a few millimeters. B1I and B3I signals are selected in the processing procedure for BDS-3. The PPP processing strategies are summarized in Table 2. Since the relevant phase biases are not provided in the PPP-B2b service, the results are given in ambiguity-float solutions.

Results and analysis

The qualities of the OSB, satellite orbit and clock offset products in PPP-B2b are presented in this section. The SISRE and orbit-only SISRE are computed and analyzed for all satellites. Positioning tests are carried out to verify the real positioning performance of the PPP-B2b service, and the results for CNES products are given for comparison.

OSB evaluation

OSB products are decoded only for the BDS-3 constellation with the same value during the analysis period in PPP-B2b. For comparison with the CAS DCB products, we convert the OSB products into DCB pairs with the reference B3I. The common DCBs for these two products are B1I-B3I, B1C(P)-B3I and B2a(P)-B3I, whereas CAS provides only B1C(P)- and B2a(P)-B3I products for C19–C37 at present. Figure 5 plots both the PPP-B2b DCBs and the CAS DCBs as well as their differences for each satellite. The two series relatively overlap for all DCB types. We further compute the STDs of the differences for all satellites between the PPP-B2b products and the CAS DCB products. The stabilities

Table 2 Processing strategies for real-time PPP

	Processing strategies
Observation type	IF-B1/B3, IF-L1/L2
Sample	30 s
Cut-off	10°
Solid tide, ocean tide	IERS Conventions 2010
PCO/PCV	IGS14.atx
Satellite orbit/clock	PPP-B2b/CNES products
Troposphere	Saastamoinen model + random walk estimation
Observation noise/PPP-B2b	GPS:4 m/0.02 m BDS-3:2 m/0.02 m for code and phase
Observation noise/CNES	GPS:2 m/0.02 m BDS-3:2 m/0.02 m for code and phase
Ambiguity	Float

of the B1C(P)- and B2a(P)-B3I DCB differences for the BDS-3 constellation are 0.29 ns and 0.24 ns, respectively, approximately 1–2 times the mean square error of the stability for the CAS BDS DCB products (0.17 ns), while the B1I-B3I DCB difference exhibits larger errors with an STD of 0.52 ns.

Orbit comparison

Figures 6 and 7 illustrate the orbit errors in the RAC directions for the PPP-B2b and CNES RTS products taking the final WUM products as a reference. In the case of the GPS constellation, the radial component has a minimum difference for the PPP-B2b products, with all satellites exhibiting errors within 0.1 m. In contrast, the errors on the along- and cross-track components are relatively large for all satellites, three to four times that in the radial direction, as summarized in Table 3. For the CNES products, the RMS values of the GPS orbit errors are very consistent in all three RAC directions with accuracies of 0.024 m (R), 0.030 m (A) and 0.024 m (C), which are much better than those of the PPP-B2b products, especially in the along- and cross-track directions. This may be because the PPP-B2b service processes only the observations from a regional GNSS network in China, while CNES uses a global network. In the case of the BDS-3 constellation, the accuracies of the radial and

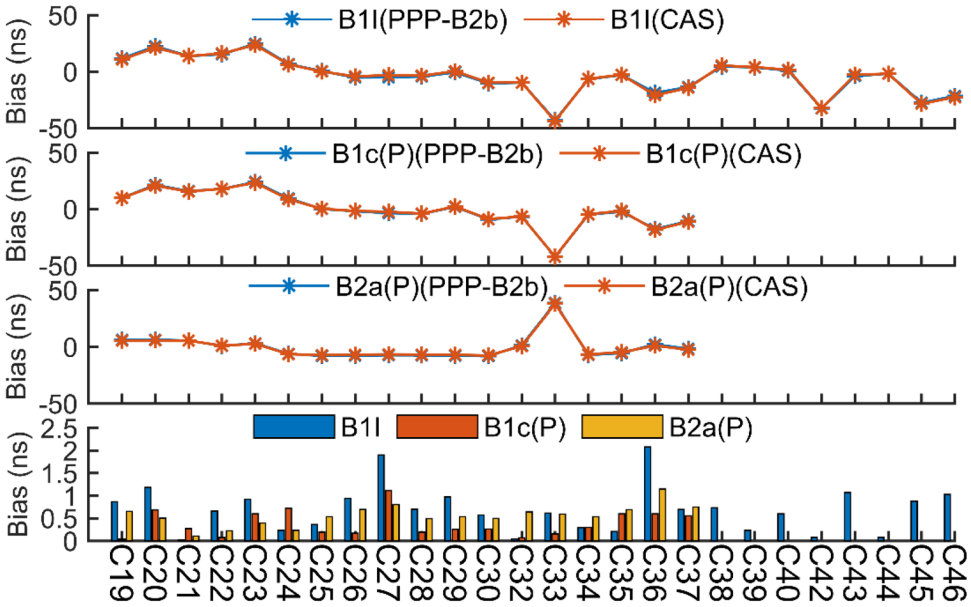

Fig. 5 Comparison of the PPP-B2b DCB and MGEX DCB for B1I-, B1C(P)- and B2a(P)-B3I. The first three graphs show the DCB value for both PPP-B2b DCB and MGEX DCB products. The bottom graph shows the difference between the two products

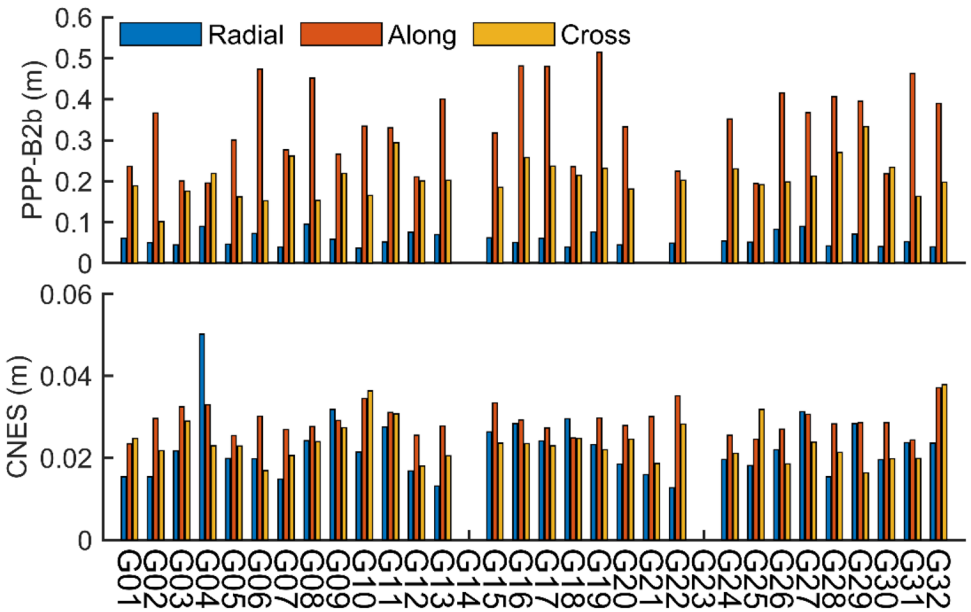

Fig. 6 GPS orbit errors for the PPP-B2b and CNES products in radial, along-track and cross-track directions with respect to the WUM post-processing products

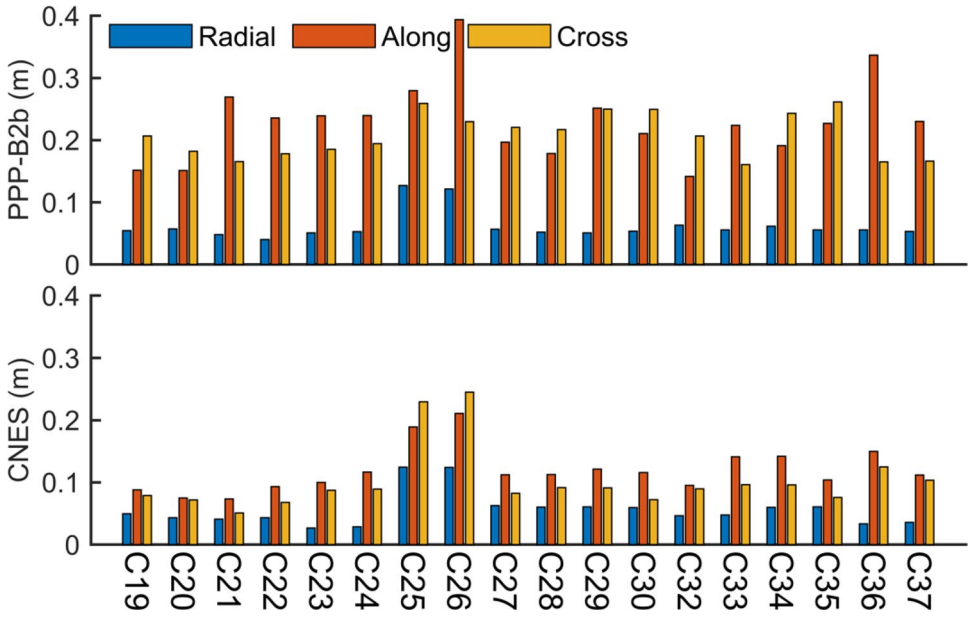

Fig. 7 BDS-3 orbit errors for the PPP-B2b and CNES products in radial, along-track and cross-track directions with respect to the WUM post-processing products

Table 3 Average RMS PPP-B2b and CNES orbit errors in radial, along-track and cross-track directions with respect to the WUM post-processing products (unit: m)

System	PPP-B2b			CNES		
	Radial	Along-track	Cross-track	Radial	Along-track	Cross-track
GPS	0.062	0.345	0.213	0.024	0.030	0.024
BDS-3	0.065	0.240	0.210	0.065	0.125	0.121

cross-track components are comparable to those of the GPS constellation in the PPP-B2b products, while BDS-3 is more accurate in the along-track direction. This difference may be due to the additional observations of the ISL terminals equipped on the BDS-3 satellites, as these terminals help improve the orbit determination, especially in the along-track direction (Tang et al. 2018). For the CNES products, the accuracy on the radial component is within 0.1 m for all BDS-3 satellites, except C25 and C26, as found using the PPP-B2b BDS-3 products. Furthermore, the accuracies of all three components are much lower than those of GPS due to the poor distribution of the MGEX BDS-3 tracking stations to date.

Clock error

The evaluation of clock products follows a DD process. The top panels of Figs. 8 and 9 display the unedited DD series for the PPP-B2b clock products on DOY 241. The sequences frequently truncate due to the satellites entering and exiting the network, especially for GPS, since some GPS satellite corrections are occasionally missing. For comparison, the bottom panels of Fig. 8 and Fig. 9 demonstrate the same series after editing using (6). These sequences confirm that systematic jumps have been removed, and thus, the series can properly reflect the accuracy. With 20 min as the limit for the loss of lock time, which is the same gap value for resetting ambiguities when observations are lost, the edited series are split into many arcs for the 7-day period. The average RMS and STD values for these arcs are calculated and compared with the CNES product, as depicted in Fig. 10.

The mean and maximum RMS clock errors for the PPP-B2b GPS products in the analysis period are 3.5 ns and 7.1 ns, respectively, while the same statistics for the CNES products are 0.3 ns and 0.6 ns. The nonzero mean satellite-specific bias degrades the precision of the pseudorange observations and enlarges the convergence time but does not impact the accuracy after convergence since the bias is absorbed into the range residuals and ambiguities during PPP. Such large RMS values in the PPP-B2b GPS products may come from the incompleteness of the network distribution used to generate the PPP-B2b RTS corrections. The initial clock offsets could not be accurately separated from the ambiguities by utilizing a regional network. However, for the PPP-B2b BDS-3 products, the average RMS statistic is 1.5 ns, which may benefit from ISL observations, and the RMS of the CNES BDS-3 clock products is 0.5 ns. For the STD statistic, which nearly determines the final PPP accuracy, the average accuracy for the PPP-B2b GPS products is 0.13 ns, which is worse than that of CNES (0.07 ns), while the PPP-B2b BDS-3 products have a better STD (0.11 ns) than the CNES RTS products (0.21 ns).

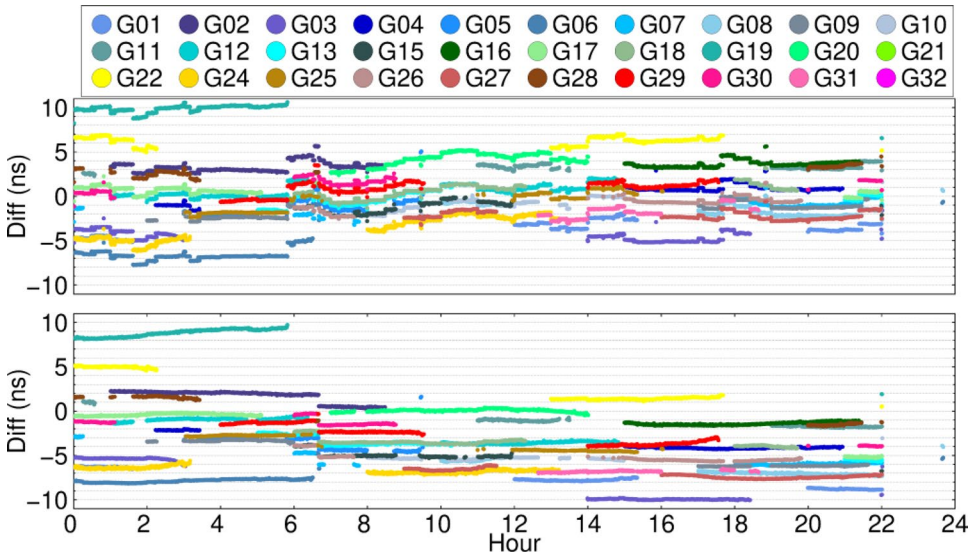

Fig. 8 DD series of PPP-B2b products with (top) and without (bottom) jumps removed for GPS. DD series are truncated due to the different reference satellite, jumps should be removed before evaluating STD statistics

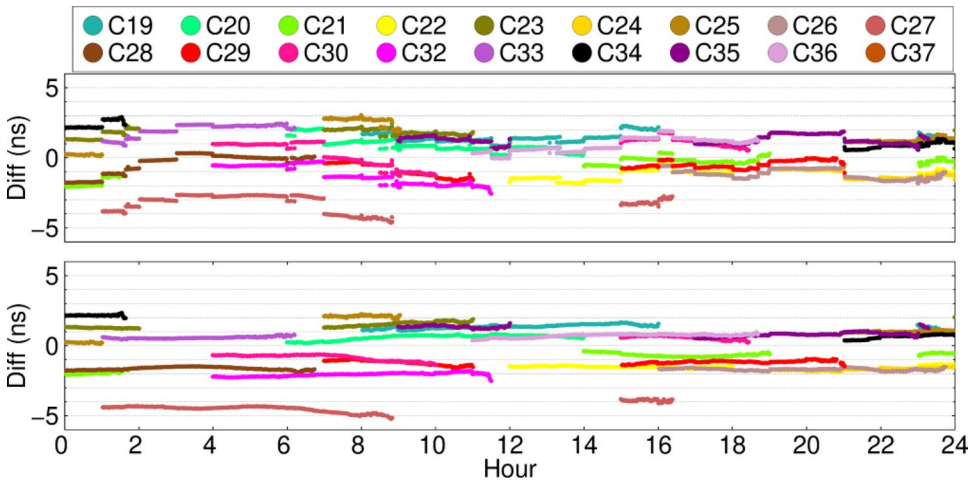

Fig. 9 DD series of PPP-B2b products with (top) and without (bottom) jumps removed for BDS-3. DD series are truncated due to the different reference satellite, jumps should be removed before evaluating STD statistics

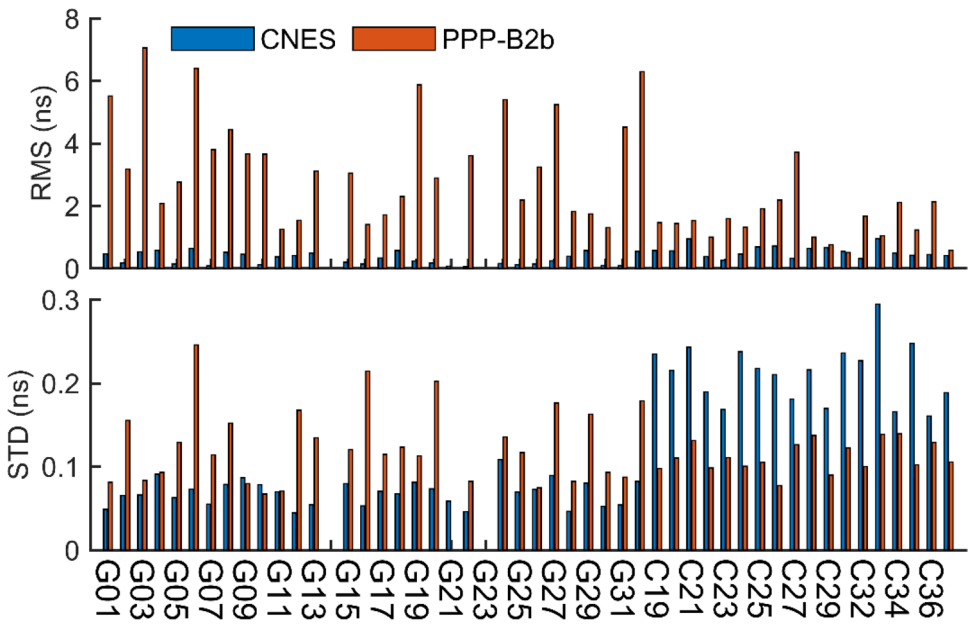

Fig. 10 RMS and STD values of the satellite clock offset errors for the CNES and PPP-B2b products

SISRE assessment

The SISREs and their STDs for the PPP-B2b and CNES RTS products are computed during the analysis period. In the case of PPP-B2b, as summarized in Table 4, the GPS constellation exhibits a large SISRE of 0.92 m±0.033, which is even worse than that of GPS navigation messages (0.6 m), while the SISRE for BDS-3 is 0.45 m±0.031, slightly better than that of BDS-3 navigation messages (Montenbruck et al. 2015; Lv et al. 2020; Shi et al. 2020). For the CNES products, the SISREs for GPS and BDS-3 are much better than those for the PPP-B2b products having values of 0.081 ± 0.012 m and 0.174 ± 0.053 m, respectively.

To determine the contributions of orbit and clock errors to the SISRE, we compute the orbit-only SISRE and clock error for each satellite, and the results are depicted in Fig. 11 and Fig. 12. The clock errors dominate the SISRE for every satellite in PPP-B2b, while the orbit-only SISRE is less than 0.06 m for all GPS and BDS-3 satellites except C25 and C26. A large pseudorange SISRE will raise the convergence time for PPP users, which has an adverse impact on real-time applications. Therefore, the satellite-specific bias in PPP-B2b clock products must be improved and corrected in future.

The STD of the SISRE series for every satellite is also analyzed in this study. When phase observations are used, the offset in the SISRE can be absorbed into the ambiguity parameters, thereby reducing their adverse impact on the positioning performance; as a result, it is possible to employ the STD to represent the actual PPP accuracy. The average STDs of the GPS and BDS-3 constellations for the PPP-B2b products are approximately 0.033 m and 0.031 m, respectively; for the CNES products, the STD values are below 0.020 m for all GPS satellites, but BDS-3 satellites exhibit larger errors of 0.053 m on average.

Table 4 Average RMS and STD values of the SISRE for the PPP-B2b and CNES products (unit: m)

	PPP-B2b		CNES	
	GPS	BDS-3	GPS	BDS-3
RMS				
SISRE	0.925	0.455	0.081	0.174
SISRE-orbit	0.052	0.055	0.020	0.055
STD				
SISRE	0.033	0.031	0.012	0.053

PPP evaluation

Several stations distributed with relative uniformity throughout China (Fig. 4) are selected for positioning tests. Experiments with GPS-only, BDS-3-only and GPS + BDS-3 observations are performed to verify the PPP-B2b service, and the results and analysis are presented and compared with those for the CNES products in the following.

Positioning accuracy

Figures 13 and 14 show the kinematic PPP series utilizing the PPP-B2b and CNES products, respectively, of representative station ZJ01 in eastern China on DOY 241. The corresponding series of the number of satellites and position dilution of precision (PDOP) for PPP-B2b and CNES are plotted in Figs. 15 and 16, respectively. For PPP-B2b,

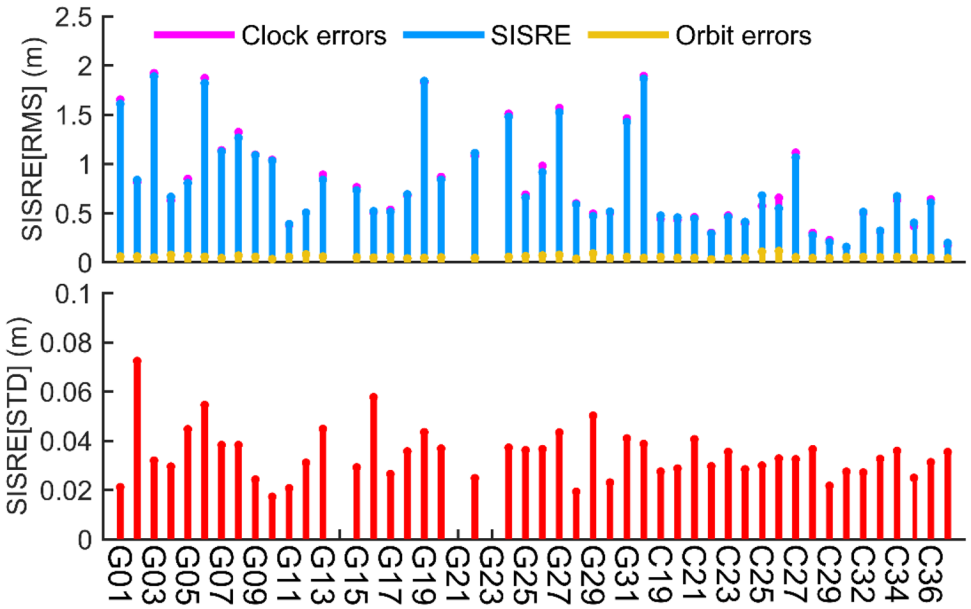

Fig. 11 SISRE statistics for GPS and BDS-3 satellites for the PPP-B2b products. The x-axis is labeled every two satellites

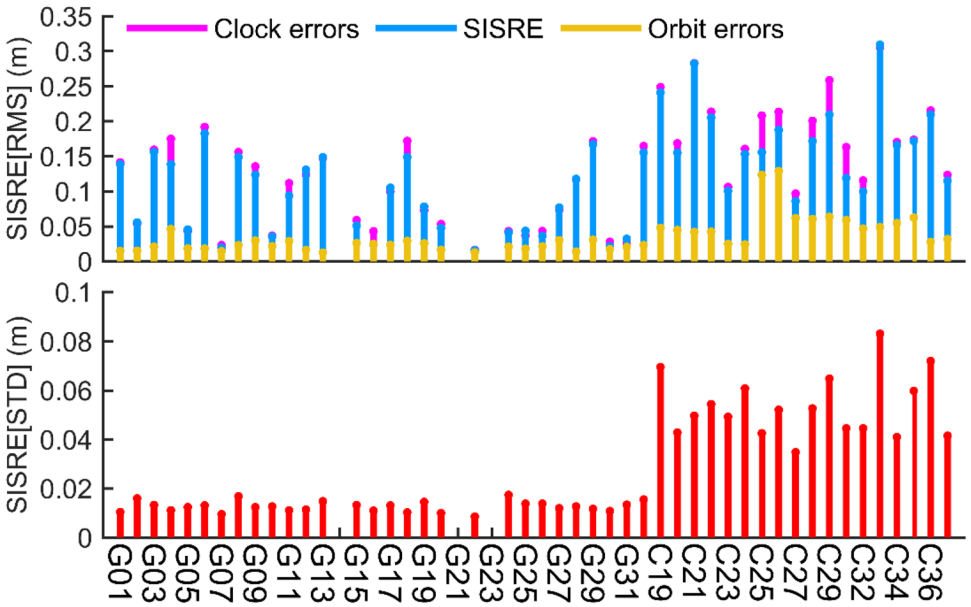

Fig. 12 SISRE statistics for GPS and BDS-3 satellites for the CNES products. The x-axis is labeled every two satellites

the PPP accuracy of BDS-3-only is 0.029/0.019/0.081 m in the east/north/up (E/N/U) directions, which is much better than that of GPS-only with 0.105/0.091/0.160 m. The average number of SSR-matched satellites on this day for GPS is 6.49, 20% lower than that for BDS-3 (8.25), which can also explain the discontinuous and large RMS values for the GPS-only solutions. The period within 22:00–24:00 is not involved in the analysis to generate the average number of satellites for GPS. The PDOP value for BDS-3 is better than that for GPS-only for almost the entire day, except during 08:00–10:00 and 20:00–22:00, whereas the PPP performance of GPS-only is comparable to that of BDS-3 during these periods. The GPS + BDS-3 solution reaches the best accuracy of 0.021/0.014/0.065 m, which is improved by 27%/26%/20% compared with the accuracy of the BDS-3-only solution. For the CNES products, in contrast, the GPS-only solution is much better than the BDS-3-only solution. The E and N accuracies of the CNES GPS-only solution are comparable to those of the PPP-B2b BDS-3-only solution, and both solutions have the same average number of matched satellites, but the former solution has a better accuracy in the U direction than the latter. This is not surprising since the CNES GPS products have smaller and more stable SISREs. The average number of available BDS-3 satellites is 5.24, which meets the minimum number of satellites for positioning because the CNES products provide

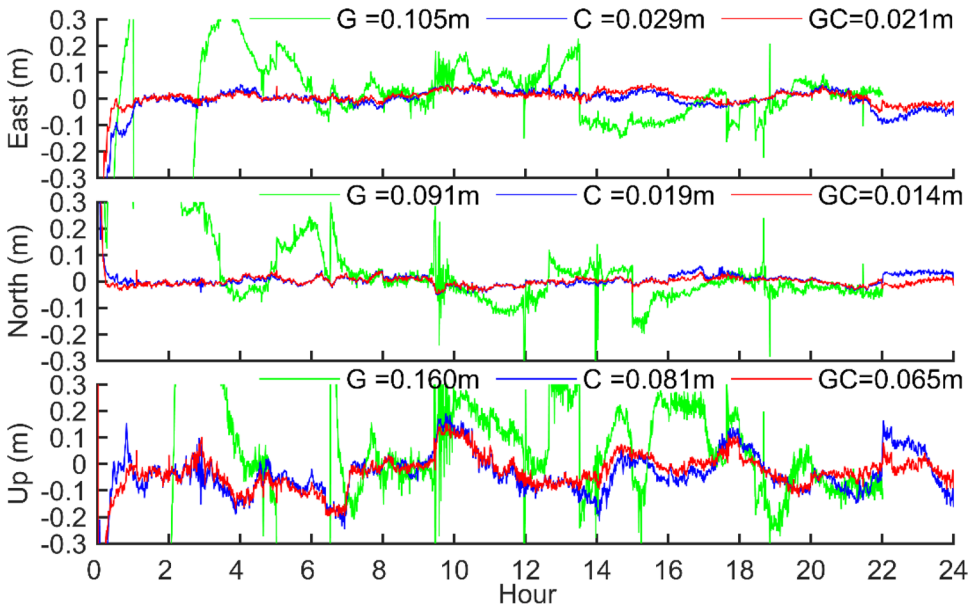

Fig. 13 PPP series of ZJ01 for different positioning modes applying PPP-B2b products. Green or 'G' stands for the GPS-only results, blue or 'C' stands for the BDS-3-only results, red or 'GC' stands for the GPS + BDS-3 combined results

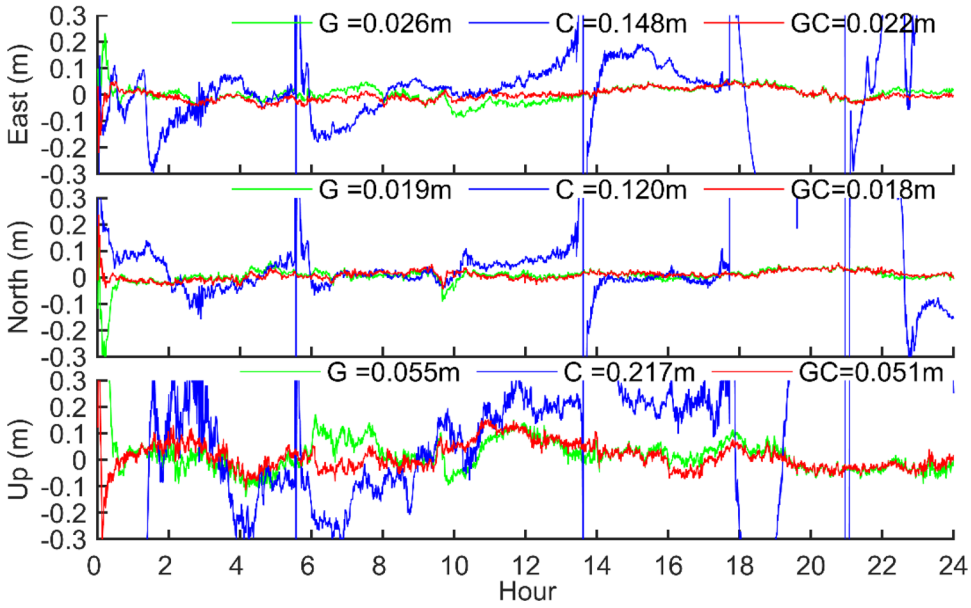

Fig. 14 PPP series of ZJ01 for different positioning modes applying CNES products. Green or 'G' stands for the GPS-only results, blue or 'C' stands for the BDS-3-only results, red or 'GC' stands for the GPS + BDS-3 combined results

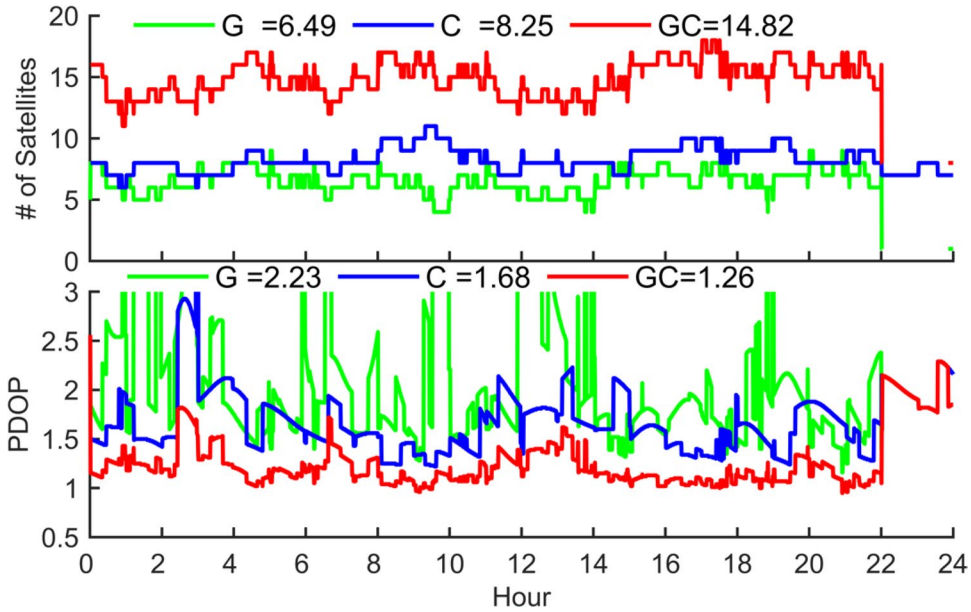

Fig. 15 Number of satellites and PDOP series for different positioning modes applying PPP-B2b products. Green or 'G' stands for the GPS-only mode, blue or 'C' stands for the BDS-3-only mode, red or 'GC' stands for the GPS + BDS-3 mode

only C19–C37 for the BDS-3 constellation. The PPP-B2b GPS-only solution exhibits the same pattern due to the lack of satellites. The accuracy is also improved after combining GPS and BDS-3 observations. In general, these results show that the PPP-B2b BDS-3 products have the same positioning service capabilities as the CNES GPS products; however, the GPS products still need to be improved.

Figures 17 and 18 show the average available number of satellites and the kinematic and static PPP solutions in the E, N and U directions with GPS-only, BDS-only and GPS + BDS-3 observations using the selected stations in Fig. 4 during the analysis period. The kinematic PPP performance for these stations follows the same pattern as that demonstrated by ZJ01. For static PPP, centimeter-level accuracy is achieved for both GPS-only and BDS-3-only observations using the PPP-B2b and CNES products, while the best accuracy is obtained with GPS + BDS-3 observations for all stations.

Convergence analysis

Defined as the time for the E/N position errors to fall and remain within 0.1 m and the U position error to fall and remain within 0.2 m, the convergence time for static PPP is analyzed for these stations in different processing modes. The parameters are programmed to reset every 4 h, and the

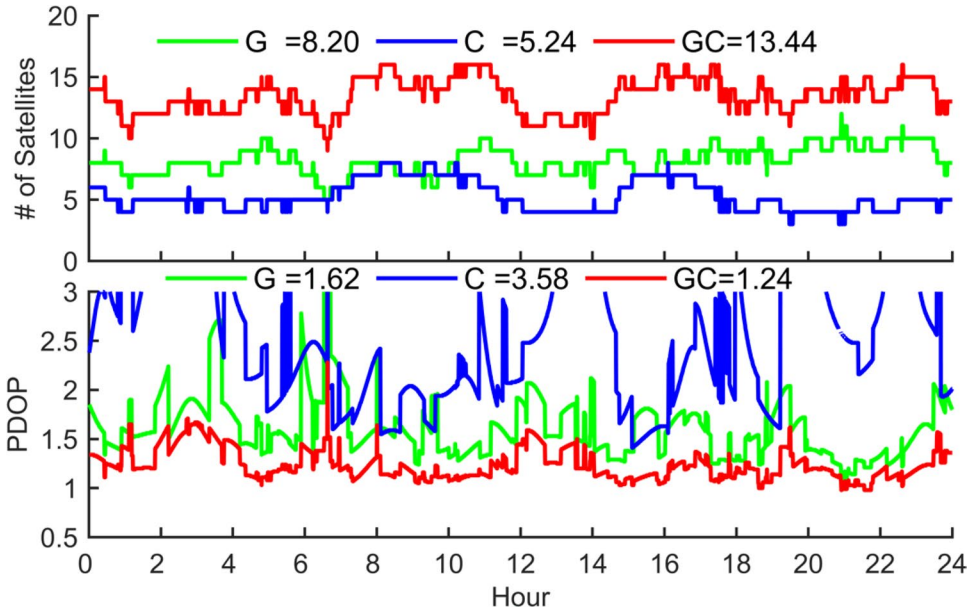

Fig. 16 Number of satellites and PDOP series for different positioning modes applying CNES products. Green or 'G' stands for the GPS-only mode, blue or 'C' stands for the BDS-3-only mode, red or 'GC' stands for the GPS + BDS-3 mode

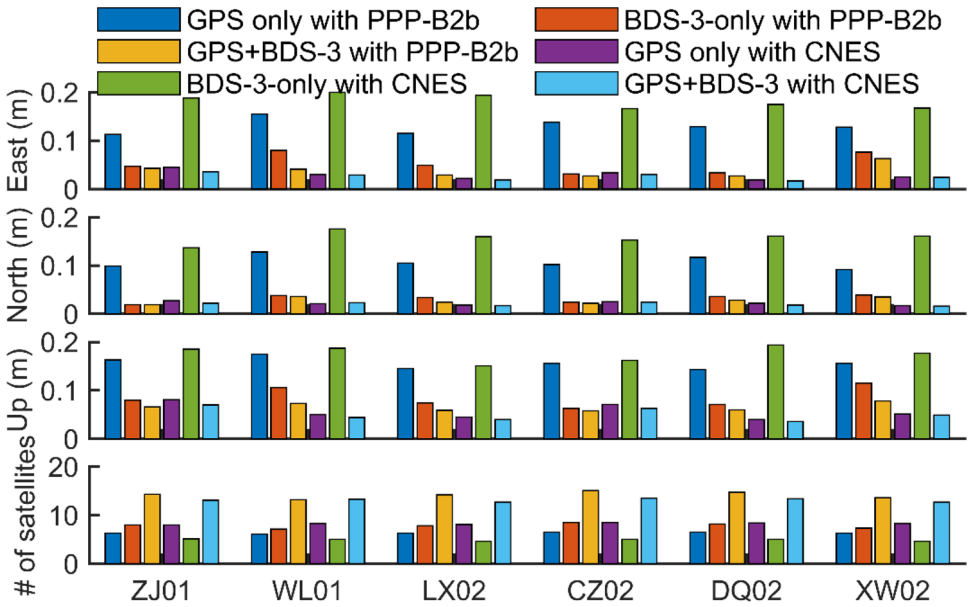

Fig. 17 Seven-day mean RMS values of the kinematic PPP solutions and the mean matched satellite numbers for different positioning modes applying PPP-B2b and CNES products

average convergence time is calculated. The results obtained by applying the PPP-B2b products are plotted in the top panel of Fig. 19. The GPS-only solution needs more than 60 min for convergence except for CZ02, while the average time for BDS-3 is only 25.3 min. The processing mode combining GPS and BDS-3 shortens the convergence time by 15.3% compared with BDS-3-only. For the results obtained applying the CNES products plotted in the bottom panel of Fig. 19, the GPS-only and BDS-3-only modes are completely opposite to the results of the PPP-B2b products, and the average convergence times for GPS and BDS-3 are 21.3 and 40.3 min, respectively.

Conclusions

To meet the demands of RTPPP, in 2020, BDS-3 initiated an RTPPP service using the B2b signal for users in China and its surrounding areas. In this study, the accuracy of PPP-B2b corrections is assessed for the GPS and BDS-3 constellations in comparison with the CNES RTS.

Based on the collected 7-day corrections, availabilities of 91.5% and 97.5% are obtained for the GPS and BDS-3 satellites, respectively, for PPP-B2b. Compared with the MGEX final DCB products provided by the University of the Chinese Academy of Sciences (CAS), the quality of

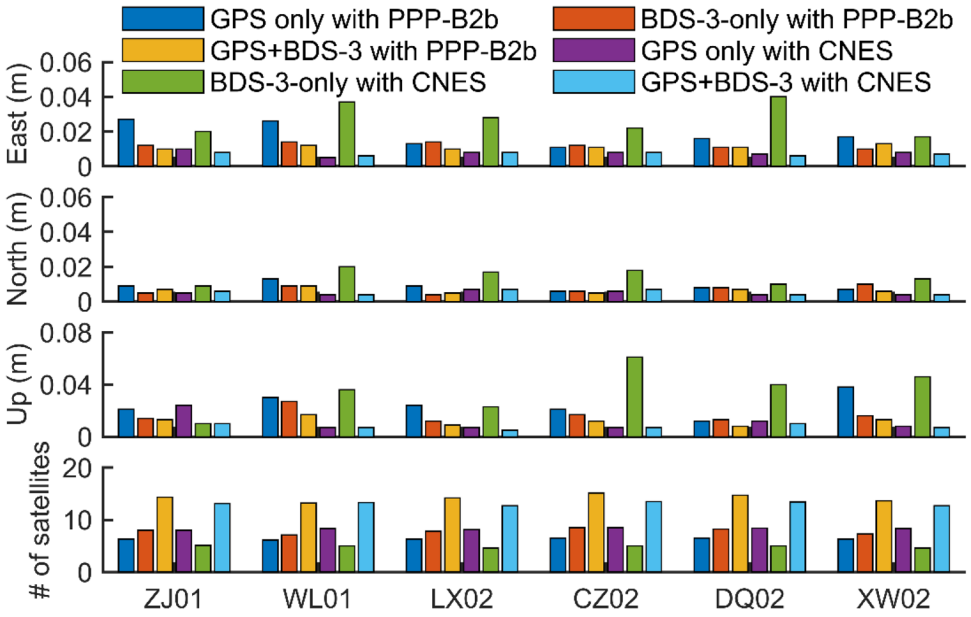

Fig. 18 Seven-day mean RMS values of the static PPP solutions and the mean matched satellite numbers for different positioning modes applying PPP-B2b and CNES products

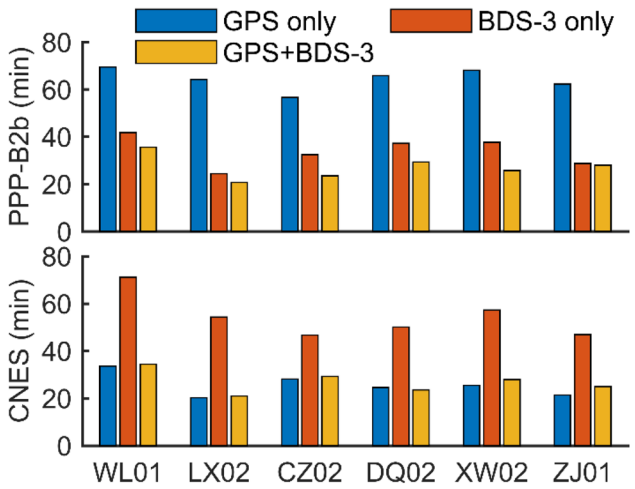

Fig. 19 Convergence times for the six stations with the PPP-B2b and CNES products in static PPP

the PPP-B2b OSB products is first evaluated. Considering the uncertainty of 0.17 ns for the CAS products, the OSBs provided by PPP-B2b show comparable performance, and the STDs are 0.52 ns, 0.29 ns and 0.24 ns for B1I, B1C and B2a, respectively. Next, the precise satellite orbits and clock offsets provided by the PPP-B2b and CNES products are evaluated in reference to the multi-GNSS products of WHU (WUM) final products. The radial component exhibits centimeter-level accuracy for both GPS and BDS-3 orbit products in PPP-B2b and CNES. Because of the ISL terminals installed on the BDS-3 satellites, the accuracy of the along-track component for the BDS-3 orbit information provided by PPP-B2b is superior to that for GPS, and the precision on the cross-track and radial components is comparable between BDS-3 and GPS. In terms of the clock error, a large average RMS error of 3.5 ns for GPS satellites is observed for the PPP-B2b products, which is much larger than that observed for the CNES products with a corresponding RMS of 0.3 ns. This is likely because the initial clock offset could not be accurately separated from the ambiguities by utilizing a regional network. Considering the orbit and clock errors, the hybrid SISRE is also computed. Large SISREs of 0.92 m$\pm$0.033 and 0.45 m$\pm$0.031 are obtained for GPS and BDS-3, respectively, for the PPP-B2b products. However, the orbit-only SISRE is less than 0.06 m for all GPS and BDS-3 satellites, except C25 and C26, which indicates that the clock errors dominate the SISRE for every satellite in PPP-B2b. Nevertheless, the STD of the SISRE is 0.03 m for both GPS and BDS-3 in PPP-B2b, which is consistent with the SISRE STD in the CNES products, with accuracies of 0.012 and 0.053 m for GPS and BDS-3, respectively.

Finally, positioning experiments with GPS-, BDS-3-only and GPS + BDS-3 observations are conducted for both the PPP-B2b and the CNES products. The best PPP performance is observed in the GPS + BDS-3 solution; the accuracy on the horizontal components is better than 5 cm and the accuracy on the vertical component is better than 10 cm for both products. The static PPP results confirm that a centimeter-level accuracy can be achieved with the PPP-B2b service, which is comparable to the CNES products. Considering the inferior performance of the GPS SISRE in the PPP-B2b service, the average convergence time of GPS-only mode in static PPP utilizing the PPP-B2b products is longer (64.4 min) than that of BDS-3-only mode (25.3 min) using the same products. According to our analysis, the PPP-B2b PPP service is comparable to the CNES RTS, and improved

RTPPP performances are expected with decreasing GPS SISRE in future.

Acknowledgment This work was sponsored by the funds of the National Natural Science Foundation of China (Grant Nos. 42030109, 41774007), the Fundamental Research Funds for the Central Universities (2042021kf0064) and the Foundation supported by Wuhan Science and Technology Bureau (2020010601012186). The authors would like to thank the IGS Multi-GNSS Experiment (MGEX), CAS, CNES, for providing relevant products and CNOSTAR Co., Ltd., for providing GNSS observations, all of which enable this study.

Data availability The PPP-B2b corrections can be obtained from the three BDS-3 GEO B2b signals, and binary data should be decoded according to the PPP-B2b ICD of BDS-3. The CNES corrections can be obtained from the IGS real-time service. Detailed information can be found on https://www.igs.org/rts/user-access/. Relevant reference products are available on https://cddis.nasa.gov. Stations for PPP validation are maintained by CNOSTAR Co., Ltd. Measurements can be obtained under permission.

References

CSNO (2017a) BeiDou Navigation Satellite System Signal In Space Interface Control Document Open Service Signal B1C (Version 1.0)

CSNO (2017b) BeiDou Navigation Satellite System Signal In Space Interface Control Document Open Service Signal B2a (Version 1.0)

CSNO (2018) Development of the BeiDou Navigation Satellite System (Version 3.0)

CSNO (2019a) Development of the BeiDou Navigation Satellite System (Version 4.0)

CSNO (2019b) The Application Service Architecture of BeiDou Navigation Satellite System (Version 1.0)

CSNO (2020a) BeiDou Navigation Satellite System Signal In Space Interface Control Document Open Service Signal B2b (Version 1.0)

CSNO (2020b) BeiDou Navigation Satellite System Signal In Space Interface Control Document Precise Point Positioning Service Signal PPP-B2b (Version 1.0)

Guo J, Xu X, Zhao Q, Liu J (2016) Precise orbit determination for quad-constellation satellites at Wuhan University: strategy, result validation, and comparison. J Geod 90(2):143–159. https://doi.org/10.1007/s00190-015-0862-9

Guo L, Wang F, Gong X, Sang J, Liu W, Zhang W (2020) Initial results of distributed autonomous orbit determination for Beidou BDS-3 satellites based on inter-satellite link measurements. GPS Solut 24(3):72. https://doi.org/10.1007/s10291-020-00985-0

Hadas T, Bosy J (2015) IGS RTS precise orbits and clocks verification and quality degradation over time. GPS Solut 19(1):93–105. https://doi.org/10.1007/s10291-014-0369-5

He C, Lu X, Guo J, Su C, Wang W, Wang M (2020) Initial analysis for characterizing and mitigating the pseudorange biases of BeiDou navigation satellite system. Satell Navig 1(1):3. https://doi.org/10.1186/s43020-019-0003-3

Kazmierski K, Zajdel R, Sośnica K (2020) Evolution of orbit and clock quality for real-time multi-GNSS solutions. GPS Solut 24(4):111. https://doi.org/10.1007/s10291-020-01026-6

Liu L, Zhang T, Zhou S, Hu X, Liu X (2019) Improved design of control segment in BDS-3. Navigation 66(1):37–47. https://doi.org/10.1002/navi.297

Lu X, Chen L, Shen N, Wang L, Jiao Z, Chen R (2020) Decoding PPP Corrections from BDS B2b signals using a software-defined receiver: an initial performance evaluation. IEEE Sens. https://doi.org/10.1109/JSEN.2020.3022622

Lv Y, Geng T, Zhao Q, Liu J (2018) Characteristics of BeiDou-3 experimental satellite clocks. Remote Sens 10(11):1847. https://doi.org/10.3390/rs10111847

Lv Y, Geng T, Zhao Q, Xie X, Zhou R (2020) Initial assessment of BDS-3 preliminary system signal-in-space range error. GPS Solut 24(1):16. https://doi.org/10.1007/s10291-019-0928-x

Montenbruck O, Steigenberger P, Hauschild A (2015) Broadcast versus precise ephemerides: a multi-GNSS perspective. GPS Solut 19(2):321–333. https://doi.org/10.1007/s10291-014-0390-8

Montenbruck O et al (2017) The Multi-GNSS Experiment (MGEX) of the International GNSS Service (IGS) – Achievements, prospects and challenges. Adv Space Res 59(7):1671–1697. https://doi.org/10.1016/j.asr.2017.01.011

Pan L, Li X, Yu W, Dai W, Kuang C, Chen J, Chen F, Xia P (2020) Performance evaluation of real-time precise point positioning with both BDS-3 and BDS-2 observations. Sensors 20(21):6027. https://doi.org/10.3390/s20216027

Shi J, Ouyang C, Huang Y, Peng W (2020) Assessment of BDS-3 global positioning service: ephemeris, SPP, PPP, RTK, and new signal. GPS Solut 24(3):81. https://doi.org/10.1007/s10291-020-00995-y

Tang C et al (2018) Initial results of centralized autonomous orbit determination of the new-generation BDS satellites with inter-satellite link measurements. J Geod 92(10):1155–1169. https://doi.org/10.1007/s00190-018-1113-7

Wang N, Yuan Y, Li Z, Montenbruck O, Tan B (2016) Determination of differential code biases with multi-GNSS observations. J Geod 90(3):209–228. https://doi.org/10.1007/s00190-015-0867-4

Wang L, Li Z, Ge M, Neitzel F, Wang X, Yuan H (2019) Investigation of the performance of real-time BDS-only precise point positioning using the IGS real-time service. GPS Solut 23(3):66. https://doi.org/10.1007/s10291-019-0856-9

Wu Z, Zhou S, Hu X, Liu L, Shuai T, Xie Y, Tang C, Pan J, Zhu L, Chang Z (2018) Performance of the BDS3 experimental satellite passive hydrogen maser. GPS Solut 22(2):43. https://doi.org/10.1007/s10291-018-0706-1

Xie X, Geng T, Zhao Q, Liu J, Wang B (2017) Performance of BDS-3: measurement quality analysis. Precise Orbit and Clock Determination Sensors 17(6):1233. https://doi.org/10.3390/s17061233

Xie X, Geng T, Zhao Q, Lv Y, Cai H, Liu J (2020) Orbit and clock analysis of BDS-3 satellites using inter-satellite link observations. J Geod 94(7):64. https://doi.org/10.1007/s00190-020-01394-4

Yang D, Yang J, Li G, Zhou Y, Tang C (2017) Globalization highlight: orbit determination using BeiDou inter-satellite ranging measurements. GPS Solut 21(3):1395–1404. https://doi.org/10.1007/s10291-017-0626-5

Yang Y, Xu Y, Li J, Yang C (2018) Progress and performance evaluation of BeiDou global navigation satellite system: Data analysis based on BDS-3 demonstration system. Sci China Earth Sci 61(5):614–624. https://doi.org/10.1007/s11430-017-9186-9

Yang Y, Mao Y, Sun B (2020) Basic performance and future developments of BeiDou global navigation satellite system. Satell Navig 1(1):1. https://doi.org/10.1186/s43020-019-0006-0

Zhang X, Wu M, Liu W, Li X, Yu S, Lu C, Wickert J (2017) Initial assessment of the COMPASS/BeiDou-3: new-generation navigation signals. J Geod 91(10):1225–1240. https://doi.org/10.1007/s00190-017-1020-3

Zhang W, Yang H, He C, Wang Z, Shao W, Zhang Y, Wang J (2020) Initial performance evaluation of precise point positioning with triple-frequency observations from BDS-2 and BDS-3 satellites. J Navig 73:763–775. https://doi.org/10.1017/S0373463319000754

Zhang Z, Li B, Nie L, Wei C, Jia S, Jiang S (2019) Initial assessment of BeiDou-3 global navigation satellite system: signal quality RTK and PPP. GPS Solut 23(4):111. https://doi.org/10.1007/s10291-019-0905-4

Jun Tao received his master's degree from Wuhan University, Wuhan, China, in 2019, where is currently a Ph.D. candidate at the School of Geodesy and Geomatics. His main research interest is real-time GNSS positioning and its application.

Jingnan Liu graduated from the former Wuhan College of Surveying and Mapping in 1967 and received his master's degree in 1982. He was elected Academician of the Chinese Academy of Engineering in 1999. Since 1998, he has been in charge of the National Engineering Research Center for Satellite Positioning System. He has been a member of the Science and Technology Committee, Ministry of Education of China in 1997–2009 and as an editorial board member of GPS Solutions in 1998–2000. He is currently an executive member of the council, Chinese Society for Geodesy, Photogrammetry and Cartography; the editorial board member of GPS World; and the coordinator of IGS.

Zhigang Hu is an associate professor at the GNSS Research Center, Wuhan University. He received his Ph.D. degree at Wuhan University in 2013. The focus of his current research lies in GNSS precise orbit determination and performance evaluation of BDS.

Qile Zhao is a professor at the GNSS Research Center of Wuhan University. He received his Ph.D. degree at Wuhan University in 2004. In 2006–2007, as a postdoctoral fellow, he did his postdoctoral program in DEOS, Delft University of Technology, the Netherlands. His current research interests are precise orbit determination of GNSS and low earth orbit satellites and high-precision positioning using GPS, Galileo, and BDS systems.

Guo Chen is a postdoctoral researcher at the GNSS Research Center of Wuhan University. He received his doctorate degree at Wuhan University in 2019. His current research mainly focuses on multi-GNSS product combination and performance evaluation of GNSS.

Boxiao Ju is a Ph.D. candidate at the GNSS Research Center, Wuhan University. He received his B.Sc. degree in 2016 from China University of Petroleum. His current research mainly focuses on GNSS deformation monitoring.